

Emergent linear Rashba spin-orbit coupling offers fast manipulation of hole-spin qubits in germanium

Yang Liu,^{1,2} Jia-Xin Xiong^{1,2}, Zhi Wang¹, Wen-Long Ma,¹ Shan Guan,^{1,*} Jun-Wei Luo^{1,2,3,†} and Shu-Shen Li^{1,2}

¹State Key Laboratory of Superlattices and Microstructures, Institute of Semiconductors, Chinese Academy of Sciences, Beijing 100083, China

²Center of Materials Science and Optoelectronics Engineering, University of Chinese Academy of Sciences, Beijing 100049, China

³Beijing Academy of Quantum Information Sciences, Beijing 100193, China



(Received 1 September 2021; revised 9 February 2022; accepted 9 February 2022; published 28 February 2022)

The electric dipole spin resonance (EDSR) combining strong spin-orbit coupling (SOC) and electric-dipole transitions facilitates fast spin control in a scalable way, which is the critical aspect of the rapid progress made recently in germanium (Ge) hole-spin qubits. However, a puzzle is raised because centrosymmetric Ge lacks the Dresselhaus SOC, a key element in the initial proposal of the hole-based EDSR. Here, we demonstrate that the recently uncovered finite k -linear Rashba SOC of 2D holes offers fast hole-spin control via EDSR with Rabi frequencies in excellent agreement with experimental results over a wide range of driving fields. We also suggest that the Rabi frequency can reach 500 MHz under a higher gate electric field or multiple GHz in a replacement by [110]-oriented quantum wells. These findings bring a deeper understanding for hole-spin qubit manipulation and offer design principles to boost the gate speed.

DOI: [10.1103/PhysRevB.105.075313](https://doi.org/10.1103/PhysRevB.105.075313)

I. INTRODUCTION

After demonstrating the all-electrical manipulation of a single hole-spin qubit in gate-defined planar quantum dots (QDs) in germanium (Ge) quantum wells (QWs) [1], remarkably rapid progress has been made in increasing the number of coupled qubits—doubled every year [2,3]. These developments leverage the compelling properties of holes in Ge QWs [4–6] such as the following: Suppressed hyperfine interaction with nuclear sites [7,8] resulting in much longer spin coherence times [9]; free from the valley degeneracy that is a crucial challenge for the use of silicon electrons as qubits [10]; low hole effective mass that benefits the desired high tunnel rates for coupled qubits [11]; and a strong spin-orbit interaction that is an inherent relativistic effect of the heavy atom [12]. Among these properties, the strong spin-orbit interaction is most striking since it allows for electric-dipole spin resonance (EDSR) controlled by alternating electric fields [13–16], bringing about faster spin manipulation in a scalable way [2,3,5] as opposed to magnetically driven electron spin resonance (ESR) used extensively for manipulation of Si electron spin qubits [17–21].

Although EDSR mediated by intrinsic spin-orbit coupling (SOC) has been demonstrated experimentally to coherently manipulate hole spins in planar Ge QDs with driving frequencies exceeding 100 MHz [2,3,5], the underlying microscopic mechanism remains ambiguous [13,22–24]. Regarding that an alternating current (AC) electric field could induce electric-dipole transitions ($\Delta n = \pm 1$, $\Delta s = 0$), we can utilize it to drive spin-flip transitions between spin-up and spin-down

states of the lowest spin doublet if and only if they are admixtures of the $n = 0$ orbital and $n = 1$ orbital with opposite spins. Linear-in- k SOC usually offers such $\Delta n = \pm 1$ interorbital spin admixture (see Appendix A for a detailed explanation). The k -linear Rashba and Dresselhaus SOC usually provide required $\Delta n = \pm 1$ coupling for electrons confined in gate-defined planar QDs [25]. However, in common sense, these k -linear SOC terms are absent in two-dimensional (2D) holes [26–28] since they are in the heavy-hole (HH) subbands. The original EDSR proposal for their hole counterparts [13–15] thus has to rely on the k -cubic Dresselhaus SOC, considering that it can also couple the ground HH ($n = 0$) to the excited HH ($n = 1$) states as a result of in-plane wave-vector quantization in planar QDs. Unfortunately, such inversion-asymmetry-induced Dresselhaus SOC is nonexistent in centrosymmetric solids, including Si and Ge. Others have suggested that the manipulation of hole-spin qubits in Ge can be achieved based on a cubic-symmetric component of the k -cubic Rashba SOC of 2D holes using a large parameter α_3 , which is deduced from a variational analysis starting from the bulk 4×4 Luttinger Hamiltonian [23,29,30]. Under the in-plane quantum confinement in the planar QDs, this cubic-symmetric component will act as a linear term due to in-plane wave-vector quantization and thus couples the $n = 0$ ground state to the $n = 1$ first excited states. However, we should note that Refs. [23,30] all considered the out-of-plane magnetic fields instead of an in-plane magnetic field utilized in the most successful experiments [2,3]. Particularly, Ref. [30] predicts theoretically a maximum Rabi frequency of 8.4 MHz generated by the cubic component of the k -cubic Rashba SOC, which is one order of magnitude smaller than the experimentally realized 108-MHz Rabi frequency [2], while Rabi frequencies in the order of several hundred MHz in Ref. [23] require a large driving AC electric field. Meanwhile,

*shan_guan@semi.ac.cn

†jwluo@semi.ac.cn

our atomistic calculations predict that the Rashba parameter of the total k -cubic terms is 3547 meV \AA^3 at an operating electric field of 30 kV/cm , indicating the cubic-symmetric component α_3 being only 452 meV \AA^3 , which is two orders of magnitude smaller than the $\alpha_3 = 3.7 \times 10^4 \text{ meV \AA}^3$ presented in Ref. [30]. Therefore, we expect the k -cubic Rashba SOC to have a negligible contribution to the EDSR, and the experimentally accessible rapid EDSR is not yet understood.

This standing puzzle may be resolved by our recently uncovered finite k -linear Rashba SOC of 2D holes in Ge/Si QWs [31]. The Rashba SOC of 2D holes in semiconductor heterostructures and QWs was commonly believed to be the k -cubic term as the lowest order due to the $3/2$ spin angular momentum nature of the HH and the isotropic kp coupling between Γ_8^v and Γ_6^c [26,32]. However, we recently uncovered a linear Rashba SOC originating from a direct, first-order dipolar coupling of the 2D HH subbands to the applied electric field [31]. This so-called direct Rashba SOC was originally discovered in 1D holes of quantum wires, with its strength proportional to the magnitude of heavy-hole-light-hole (HH-LH) mixing at the zone center [12,33,34]. Because the zone-center HH-LH mixing is usually thought to be forbidden by symmetry, direct Rashba SOC was hence expected to be absent in [001]-oriented QWs. However, ample experimental and theoretical evidence suggests finite HH-LH mixing occurred in [001]-oriented QWs, which was argued to be originating from the local C_{2v} interface [35–38]. We indeed found linear direct Rashba SOC in [001]-oriented Ge/Si QWs by performing atomistic pseudopotential method calculations [31]. Here, relying on this emergent k -linear Rashba SOC supplying the required coupling between $\Delta n = 1$ HH states, we develop the EDSR technique for planar QD confined hole spins following Ref. [13]. Using a set of experimental device parameters with input Rashba parameter obtained from the atomistic pseudopotential method calculation without *ad hoc* assumptions, we predict a 100-MHz Rabi frequency in excellent agreement with the experimental result of 108 MHz [2]. We also reproduce the experimentally measured electric-field dependencies of Rabi frequency under two investigated magnetic fields of 0.5 and 1.65 T. Consequently, we have solved the puzzle by identifying the emergent linear Rashba SOC contributing to EDSR for rapid control of hole spins confined in planar Ge QDs.

II. THEORETICAL MODEL

The experimental setup of gate-defined planar Ge QD formed in a [001]-oriented Ge/SiGe quantum well [2,3,5] is shown schematically in Fig. 1(a) with an applied static magnetic field $\mathbf{B} = (B_x, B_y, B_z)$. Following Ref. [13], the effective Hamiltonian describing the pure HH whose effective spin is parallel or antiparallel to the magnetic field direction reads

$$H_{\text{QD}} = \frac{\pi_x^2 + \pi_y^2}{2m_{\parallel}} + U(x, y) + H_{\text{SO}} + \frac{1}{2}g\mu_B\mathbf{B} \cdot \boldsymbol{\sigma}, \quad (1)$$

where $\boldsymbol{\pi} = \mathbf{p} + e\mathbf{A}$ is the usual Peierls substitution with the vector potential \mathbf{A} , m_{\parallel} is the in-plane HH effective mass, g is the Lande g -factor tensor of HH, $\boldsymbol{\sigma}$ is the Pauli vector, and μ_B is the Bohr magneton. The harmonic lateral confining potential is $U(x, y) = \frac{1}{2}m_{\parallel}\omega_0^2(x^2 + y^2)$, where $\omega_0 = \hbar/m_{\parallel}r_0^2$

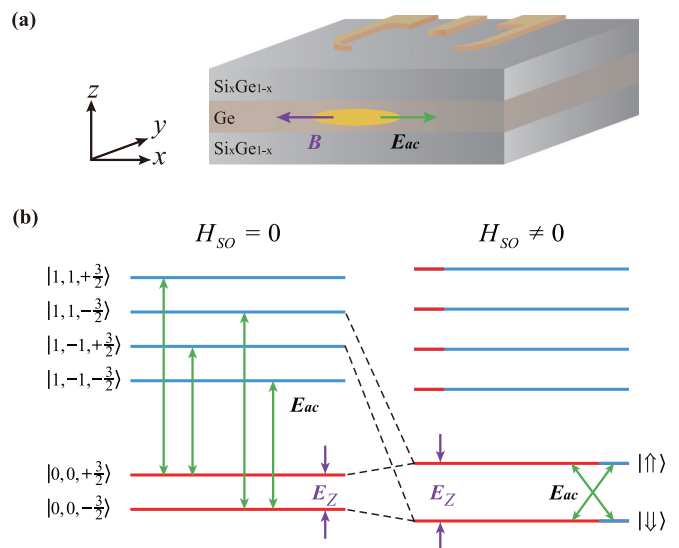


FIG. 1. (a) Schematic illustration of hole state occupying a planar QD, defined by voltage-biased gates on top of the Ge/SiGe QW. The magnetic field \mathbf{B} and AC electric field \mathbf{E}_{AC} exert on the hole state for EDSR control. (b) The k -linear Rashba SOC mixes the HH ground $n = 0$ states with the HH excited $n = 1$ states, thus making the EDSR possible. Rabi oscillations can be achieved if the in-plane AC electric field \mathbf{E}_{AC} frequency resonates with the Zeeman splitting E_Z of the lowest SOC-hybridized spin doublet.

is the energy scale that characterizes the lateral confinement for an effective QD lateral size r_0 . Here, we take a gauge $\mathbf{A} = B_z(-y/2, x/2, 0)$, considering negligible orbital effect induced by in-plane components B_x and B_y due to the strong quantization of motion along z [22,25]. In the absence of SOC ($H_{\text{SO}} = 0$), we can label the eigenstates of Eq. (1) as the product of Fock-Darwin and spin states $|n, l, s\rangle = |n, l\rangle|s\rangle$, where n, l are the principle and azimuthal quantum numbers, respectively, and $s = \pm 3/2$. Figure 1(b) shows that each level is a Kramer's doublet that splits into two spin states in a magnetic field: $E_{n,l,s} = \hbar\Omega(n+1) + \hbar\omega_L l + \hbar\omega_Z s/3$ ($\Omega = \sqrt{\omega_0^2 + \omega_L^2}$, $\omega_Z = \mu_B g \cdot \mathbf{B}/\hbar$, and $\omega_L = eB_z/2m_{\parallel}$ is the Larmor frequency). A qubit can be encoded into the lowest spin doublet. When applying an in-plane AC electric field $\mathbf{E}_{\text{AC}}(t) = E_{\text{AC}}(\sin\omega t, \cos\omega t, 0)$ created by driving gates, electric-dipole transitions ($\Delta n = \pm 1$, $\Delta s = 0$) occur between the lowest and higher excited doublets rather than within the lowest Zeeman-split spin doublet to yield spin flip.

The situation might alter taking the SOC into account ($H_{\text{SO}} \neq 0$) since it entangles the orbitals with the different spins. Because of the absence of bulk inversion asymmetry induced Dresselhaus SOC in centrosymmetric solids, structural inversion asymmetry induced Rashba effect (including interface effect) becomes the only source for SOC in Ge/Si QWs, in which a finite k -linear term instead of a (commonly thought) k -cubic term has recently been recognized as the leading order in Rashba SOC of 2D HH [31]. This k -linear Rashba SOC arises from a combination of local interface-induced HH-LH coupling and direct dipolar intersubband coupling to the external electric field. Since the k -linear term tends to overwhelm all other higher-order terms that are very

weak in Ge [24,26], the effective SOC Hamiltonian reads

$$H_{\text{SO}} = \frac{\alpha_R}{\hbar} (\pi_x \sigma_y - \pi_y \sigma_x), \quad (2)$$

where α_R is the Rashba parameter obtained from the atomistic pseudopotential calculations for Ge/Si QWs [31]. Taking H_{SO} into account as a perturbation to H_{QD} , we obtain the Zeeman-split ground spin doublet in the first-order perturbation theory as follows:

$$|0\pm\rangle = |0, 0, \pm 3/2\rangle + \beta^\pm |1, \pm 1, \mp 3/2\rangle, \quad (3)$$

where $\beta^\pm = \mp \alpha_R m_\parallel \ell \omega_\pm / \hbar \omega_\alpha^\pm$, $\ell = \sqrt{\hbar/m_\parallel \Omega}$, $\omega_\pm = \Omega \pm \omega_L$, $\omega_\alpha^- = \omega_- + \omega_Z$, and $\omega_\alpha^+ = \text{sgn}(\omega_+ - \omega_Z) \sqrt{(\omega_+ - \omega_Z)^2 + [2\alpha_R m_\parallel \ell \omega_+ / \hbar]^2}$. From Eq. (3) we learn that electric-dipole transitions between $|0, 0, -3/2\rangle$ and $|1, \pm 1, -3/2\rangle$ will bring $|0-\rangle$ (spin-down state $|\downarrow\rangle$) to $|0+\rangle$ (spin-up state $|\uparrow\rangle$), as shown in Fig. 1(b). When the frequency of the electric field matches the spin resonance frequency of the qubit, stable Rabi oscillation occurs [13].

We now turn to estimate the Rabi frequency based on the effective Hamiltonians described above, following the procedure for the electron counterpart [22,39]. The detailed derivation is given in Appendix B. Considering that the Rabi frequency is strongly dependent on the directions of static magnetic and AC electric field, we study the case under in-plane and out-of-plane magnetic fields, separately. For the case under an in-plane magnetic field $\mathbf{B} = (B_x, 0, 0)$ (we set the AC electric field along the x direction for simplicity), the Rabi frequency is as follows:

$$f_R^{B_\parallel} = \frac{eE_{\text{AC}}\alpha_R g_\parallel \mu_B B_x}{2\hbar(\hbar^2\omega_0^2 - g_\parallel^2 \mu_B^2 B_x^2)}. \quad (4)$$

For $\mathbf{B} = (0, 0, B_z)$, we obtain the Rabi frequency

$$f_R^{B_\perp} = \frac{eE_{\text{AC}}\alpha_R g_\perp \mu_B B_z}{2\hbar(\hbar\omega_- + g_\perp \mu_B B_z)(\hbar\omega_+ - g_\perp \mu_B B_z)}. \quad (5)$$

The g factor is highly anisotropic in Ge: The in-plane g factor is $g_\parallel \sim 0.3$ measured in single-hole qubit experiments [1,2]; nevertheless, the out-of-plane g factor is $g_\perp = 15.7$ [40]. To have the same Zeeman splitting and thus Rabi frequency, a much smaller magnetic field magnitude is required for the out-of-plane scenario than for the in-plane scenario.

III. RESULTS

In the following, we focus on the $\mathbf{B} = (B_x, 0, 0)$ scenario that has been adopted in recent experiments with achieved Rabi frequency exceeding 100 MHz for hole spin confined in gate-defined QDs [1–3] in strained Ge/Si_{0.2}Ge_{0.8} QW with a 16-nm-thick Ge layer [41]. Figure 2(a) shows the calculated $f_R^{B_\parallel}$ as a function of driving amplitude E_{AC} for $B = 1.65$ T and $B = 0.5$ T, respectively. To make a direct quantitative comparison with experimental results, here we calculate Rabi frequency $f_R^{B_\parallel}$ according to Eq. (4) by employing experimental parameters (taken $r_0 = 50$ nm for dot lateral size in the range 40–60 nm [1], $m_\parallel = 0.09m_0$ for Ge under an in-plane compressive strain of 0.63% [41]) except for the Rashba parameter α_R . As shown in Fig. 2(b), we predict $\alpha_R = 2.01$ meV Å by performing atomistic calculations for the corresponding Ge QW under an estimated biased electric field

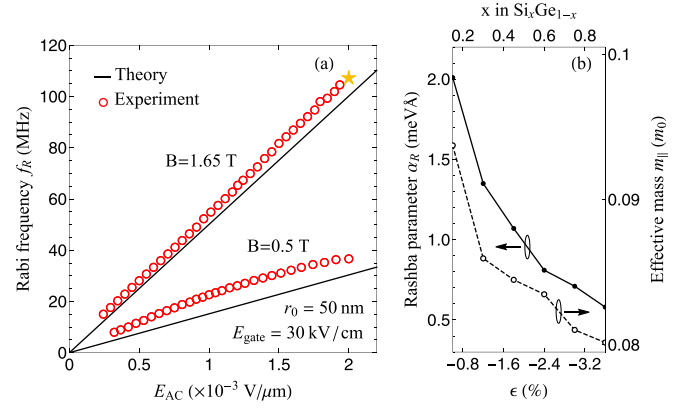


FIG. 2. (a) The theoretically predicted Rabi frequency as a function of the amplitude of the AC electric field upon application of in-plane magnetic fields of $B = 1.65$ T and $B = 0.5$ T, respectively, compared to corresponding experimental results [2] for planar Ge QD formed in a strained Ge/Si QW with Ge layer thickness of $L = 16.7$ nm. We take an effective dot radius $r_0 = 50$ nm for 40–60-nm dot lateral size in the experiment [11,41]. For comparison, we have mapped the experimental microwave power given in Ref. [2] to E_{AC} regarding the maximum microwave power was estimated corresponding to $E_{\text{AC}} = 2 \times 10^{-3}$ V/ μm [42]. (b) The predicted k -linear Rashba parameter α_R and HH in-plane effective mass m_\parallel of strained Ge QW as a function of in-plane strain ϵ by carrying out atomistic pseudopotential method calculations. Because the strain of the Ge layer is induced by the Si _{x} Ge _{$1-x$} alloy barrier, we can relate ϵ to the Si content x in the Si _{x} Ge _{$1-x$} alloy barrier by Vegard's law $\epsilon = -0.04x$ [43]. Here, we theoretically obtain $\epsilon = -0.8\%$ for Si_{0.2}Ge_{0.8} alloy barrier, but we still adopt experimentally determined $\epsilon = -0.63\%$ [41] for calculations of α_R and m_\parallel .

of 30 kV/cm for the commonly used gate voltages [42]. One can see from Fig. 2(a) that the theoretically predicted Rabi frequency is in excellent agreement with experimental results over a wide range of driving amplitude for both magnetic fields. Specifically, the fastest Rabi frequency of 108 MHz [2] was reached experimentally at $B = 1.65$ T, under which our theoretically predicted value is 100 MHz. The high agreement illustrates that the emergent k -linear Rashba SOC via EDSR provides the fast hole-spin control in planar Ge QDs.

Raising the Si content x in the Si _{x} Ge _{$1-x$} barrier will linearly enhance the compressive strain in the Ge layer [41,43] because Si has a lattice constant 4.3% smaller than that of Ge. Figure 2(b) shows that the enhanced compressive strain, in turn, causes a reduction in both Rashba parameter α_R and in-plane HH effective mass m_\parallel , which is consistent with the experimental observations [44]. The reduction in m_\parallel will benefit the enhancement of hole mobility. However, it also yields a detriment in the Rabi frequency combining with the reduction of α_R , as shown in Fig. 3(b). Hence, a low Si content in the Si _{x} Ge _{$1-x$} barrier is demanded to achieve a high Rabi frequency. It is worth noting that our atomistic pseudopotential method predicts the HH effective mass of bulk Ge to be about $0.074m_0$, in good agreement with the first-principles calculation using the mBJ functional [23]. However, different from bulk effective mass, the hole effective mass of the quantum well is predicted to be around $0.09m_0$, which is close to some experimental values [27,45–47] but deviates from the recently

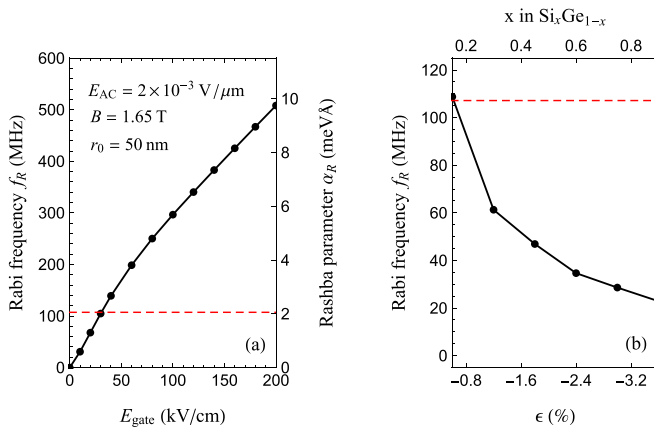


FIG. 3. (a) The predicted Rabi frequency (and k -linear Rashba parameter α_R) as a function of gate electric field for $r_0 = 50$ nm, $B = 1.65$ T, and $E_{AC} = 2 \times 10^{-3}$ V/ μm . The red dashed line indicates the maximum Rabi frequency of 108 MHz achieved experimentally [2]. (b) The corresponding Rabi frequency as a function of biaxial strain in the Ge layer.

reported value, namely $(0.048 \pm 0.006)m_0$ at zero hole density [11]. A similar discrepancy also occurs in the well-established 2D GaAs/AlGaAs heterostructures. The Princeton group [48] found that for holes in a 20-nm quantum well, the cyclotron mass decreases from $0.48m_0$ at high hole density to $0.29m_0$ at low density. However, the cyclotron mass for holes confined at a heterojunction is fairly insensitive to the density and has a value of approximately $0.5m_0$. This quantitative discrepancy is not yet understood and may be caused by the complex energy band structure of the valence bands [49].

The strength of the Rashba SOC is usually electrically tunable by biased gates, which provides a feasible way to enhance the Rabi frequency further. We examine the Rabi frequency by varying gate electric field E_{gate} applied to Ge/Si QW whose α_R is obtained from the atomistic calculations. Figure 3(a) exhibits that the Rabi frequency grows up linearly as we amplify the gate electric field due to the enhancement of Rashba SOC strength α_R . The Rabi frequency boosts to 500 MHz at a 200-kV/cm gate electric field compared with the reported 108 MHz at 30 kV/cm [2].

IV. DISCUSSION

So far, we have demonstrated that the emergent k -linear Rashba SOC drives the fast Rabi frequency achieved experimentally. However, this k -linear Rashba SOC is relatively weak ($\alpha_R < 10$ meVÅ) in [001]-oriented Ge QWs compared with [110]-oriented counterparts where α_R exceeds 120 meVÅ [50] and Ge nanowires where α_R is predicted over 400 meVÅ [12]. We thus expect that Rabi frequency can reach multiple GHz for gate-defined QDs formed in [110]-oriented Ge/Si QWs and Ge nanowires. In addition, the asymmetry in the lateral confinement potential of QDs has also been suggested to enhance Rabi frequency [42]. Besides SOC-driven EDSR, there is another mechanism contributing to EDSR. It is known as g -tensor magnetic resonance (g -TMR), which utilizes the gate-voltage modulation of a g

matrix [51,52]. Crippa *et al.* have discriminated the contributions of these two mechanisms to Rabi frequency for a Si hole-spin qubit in the nanowire and found the SOC mechanism to be the main contributor to the Rabi frequency [51]. Specifically, the g -TMR mechanism is negligible when the magnetic field is applied in plane along the nanowire direction [51] in the same configure as investigated here.

On the other hand, we note that our predicted α_3 differs significantly from that obtained by others [23,29,30] using the variational method starting from the bulk 4×4 Luttinger Hamiltonian [29] with the need to judge at the outset which selected 3D bands will couple in 2D systems. Their calculations are based on a traditional approach, where hole or electron spin physics in low-dimensional nanostructures is described by an expansion in a rather small basis of 3D bulk envelope functions [53–55]. When a basis set is restricted, the resolution of the expansion is limited and can be “farsighted” due to, e.g., the actual atomistic symmetry of the low-dimensional nanostructures being replaced by a fictitious higher symmetry [56]. In the standard model for spin splitting (SS) of nanostructures [9,26,54], this farsightedness is reflected in the use of a phenomenological Hamiltonian that requires deciding at the outset which 3D bands couple in two dimensions and, therefore, may miss important interactions that are not selected in the model Hamiltonian [28,56]. It has been demonstrated that some important properties such as zone-center HH-LH coupling [28,31], linear Dresselhaus SOC [28], and direct Rashba SOC [31] will be missed in this farsighted method due to the complex band structure of valence bands. However, the missed zone-center HH-LH coupling is essential for the emergence of the direct Rashba SOC in low-dimensional structures [12,31,34]. In the [001]-oriented QWs, the zone-center HH-LH coupling was commonly believed to be absent since it is forbidden by the QW D_{2d} symmetry [35]. But, both experiments and atomistic calculations have frequently observed the zone-center HH-LH coupling, which has now been identified as induced by the local interface C_{2v} symmetry [35,36]. In contrast, we treat the 2D nanostructure as a system in its own right and calculate the 2D band structure using the microscopic potential of the 2D system explicitly, thus freeing us from the need to judge at the outset which selected 3D bands (e.g., 4×4 Luttinger Hamiltonian in Refs. [9,23,29,30]) will couple in two dimensions. Our method has revealed a hitherto unsuspected Dresselhaus k -linear term for holes in two dimensions, which implied a different understanding of hole physics in low dimensions [28]. It thus explains why the linear direct Rashba SOC can be predicted by the atomistic pseudopotential method rather than the farsighted model Hamiltonian employed in Refs. [23,29,30]. On the other hand, the ignored remote bands in the model Hamiltonian, especially for the low-dimensional nanostructures, can also contribute to the SOC-induced splitting, thereby affecting the estimation of the strength of the k -cubic Rashba parameter. It reflects the overestimation of α_3 in Refs. [29,30] since it may be significantly canceled out considering a complete basis by including more bands.

From the above considerations, the variational method used in Refs. [23,29,30] may not accurately describe the hole states of the quantum wells, which are the platform of Ge hole

quantum computation. Instead, we adopt an all-band full-zone atomistic pseudopotential method to calculate the spin splitting of the valence subbands in semiconductor QWs, where the real QW structures, including interfaces, are considered [50]. Correspondingly, the obtained results are supposed to be more accurate than those in Refs. [23,29,30] and hence are powerful enough to describe the Rashba spin splitting in QWs.

V. CONCLUSION

In conclusion, we have resolved the standing puzzle by identifying the emergent k -linear Rashba SOC in 2D holes as the driver via EDSR for the rapid hole-spin manipulation achieved experimentally. Because the k -linear Rashba SOC is electrically tunable, we suggest using the applied gate electric field to enhance the Rabi frequency exceeding 500 MHz. We can further boost the Rabi frequency to multiple GHz if we replace the [001]-oriented Ge QW by its [110]-oriented counterpart.

ACKNOWLEDGMENTS

The work was supported by the National Science Fund for Distinguished Young Scholars under Grant No. 11925407, the

Basic Science Center Program of the National Natural Science Foundation of China (NSFC) under Grant No. 61888102, and the Key Research Program of Frontier Sciences, CAS under Grant No. ZDBS-LY-JSC019 and CAS Project for Young Scientists in Basic Research under Grant No. YSBR-026. S.G. was also supported by the NSFC under Grant No. 11904359.

APPENDIX A: FOCK-DARWIN STATES

The Fock-Darwin states are the eigenstates of the quasi-2D quantum dot. For a gate-defined planar QD with an applied static magnetic field $B = (B_x, B_y, B_z)$, without considering the SOC, the effective Hamiltonian describing a HH reads

$$H_0 = \frac{\pi_x^2 + \pi_y^2}{2m} + \frac{1}{2}m\omega_0^2(x^2 + y^2) + \frac{1}{2}g\mu_B B\sigma. \quad (\text{A1})$$

The meaning of the symbols is the same as in the main text. The eigenstates of this Hamiltonian are $|n, l, s\rangle \equiv |n, l\rangle|s\rangle$, where $|n, l\rangle$ denote the Fock-Darwin states with the principal (azimuthal) quantum number n (l).

Next, we give the derivation of the Fock-Darwin states. It is convenient to introduce phase coordinates (q_1, q_2, p_1, p_2) which are connected to the previous ones (x, y, p_x, p_y) by the following formula:

$$\begin{pmatrix} q_1 \\ q_2 \\ p_1 \\ p_2 \end{pmatrix} = \begin{pmatrix} \sqrt{\frac{\Omega}{2\omega_+}} & 0 & 0 & \frac{1}{m}\sqrt{\frac{1}{2\Omega\omega_+}} \\ \sqrt{\frac{\Omega}{2\omega_-}} & 0 & 0 & -\frac{1}{m}\sqrt{\frac{1}{2\Omega\omega_-}} \\ 0 & -m\sqrt{\frac{\Omega\omega_+}{2}} & \sqrt{\frac{\omega_+}{2\Omega}} & 0 \\ 0 & m\sqrt{\frac{\Omega\omega_-}{2}} & \sqrt{\frac{\omega_-}{2\Omega}} & 0 \end{pmatrix} \begin{pmatrix} x \\ y \\ p_x \\ p_y \end{pmatrix}, \quad (\text{A2})$$

where, $\Omega = \sqrt{\omega_0^2 + \omega_c^2/4} \equiv \sqrt{\omega_0^2 + \omega_L^2}$, $\omega_{1/2} \equiv \omega_{\pm} = \Omega \pm \omega_L$, $\omega_L = \frac{eB}{2m}$. In the new phase coordinates, H_0 has the canonical form

$$H_0 = \frac{p_1^2 + p_2^2}{2m} + \frac{m}{2}(\omega_1^2 q_1^2 + \omega_2^2 q_2^2) + \frac{1}{2}g\mu_B B\sigma. \quad (\text{A3})$$

Within second quantization, we can write

$$H_0 = \sum_{j=1}^2 \hbar\omega_j \left(a_j^\dagger a_j + \frac{1}{2} \right) + \frac{1}{2}g\mu_B B\sigma. \quad (\text{A4})$$

where the annihilation and creation operators read

$$\begin{aligned} a_1 &= \sqrt{\frac{m\Omega}{4\hbar}} \left(x + \frac{p_y}{m\Omega} - iy + i\frac{p_x}{m\Omega} \right), \\ a_2 &= \sqrt{\frac{m\Omega}{4\hbar}} \left(x - \frac{p_y}{m\Omega} + iy + i\frac{p_x}{m\Omega} \right), \\ a_1^\dagger &= \sqrt{\frac{m\Omega}{4\hbar}} \left(x + \frac{p_y}{m\Omega} + iy - i\frac{p_x}{m\Omega} \right), \\ a_2^\dagger &= \sqrt{\frac{m\Omega}{4\hbar}} \left(x - \frac{p_y}{m\Omega} - iy - i\frac{p_x}{m\Omega} \right), \end{aligned} \quad (\text{A5})$$

and the energy is given by

$$\begin{aligned} E_{n_1, n_2, s} &= (n_1 - n_2)\hbar\omega_L + (n_1 + n_2 + 1)\hbar\sqrt{\omega_0^2 + \omega_L^2} \\ &\quad + \frac{s}{3}g\mu_B B, \end{aligned} \quad (\text{A6})$$

where n_1 and n_2 are the eigenvalues of the particle number operators of the two harmonic oscillators. Introducing the main quantum number n and azimuthal quantum number $l \in \{-n, -n+2, \dots, n-2, n\}$ via $n = n_1 + n_2$ and $l = n_1 - n_2$, we can label the eigenstates as $|n, l\rangle$, which are the Fock-Darwin states. Their representation in planar polar coordinates (r, φ) reads

$$\psi_{n,l}(r, \varphi) = \sqrt{\frac{n!}{\pi(n+|l|)!}} \frac{e^{il\varphi}}{b} \left(\frac{r}{b}\right)^{|l|} L_n^{|l|} \left(\frac{r^2}{b^2}\right) e^{-r^2/2b^2}, \quad (\text{A7})$$

where $L_n^{|l|}(r^2/b^2) = (-1)^{|l|} \partial_r^{|l|} L_{n+|l|}(r^2/2b^2)$ denote the generalized Laguerre polynomials and $b^2 = \hbar/m\sqrt{\omega_0^2 + \omega_L^2}$ with Larmor frequency $\omega_L = eB/2m$.

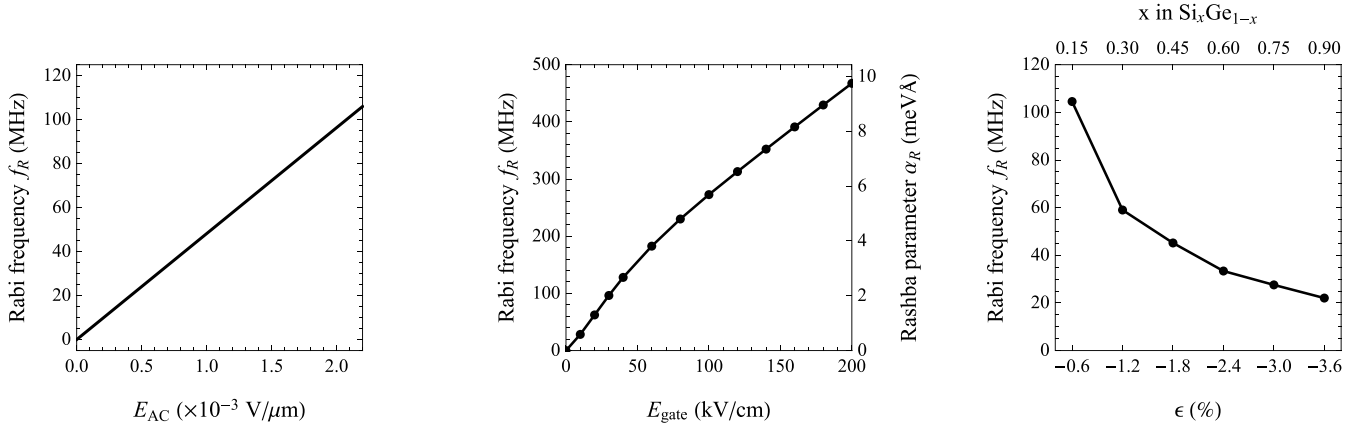


FIG. 4. The dependence of Rabi frequency on the driving electric field, the gate electric field, and the components in the presence of an out-of-plane magnetic field of 0.04 T.

We can use the annihilation and creation operators to present x , y , p_x , p_y ,

$$\begin{aligned} x &= \frac{1}{2} \sqrt{\frac{\hbar}{m\Omega}} (a_1 + a_2 + a_1^\dagger + a_2^\dagger), \\ y &= \frac{i}{2} \sqrt{\frac{\hbar}{m\Omega}} (a_1 - a_2 - a_1^\dagger + a_2^\dagger), \\ p_x &= -\frac{i}{2} m\Omega \sqrt{\frac{\hbar}{m\Omega}} (a_1 + a_2 - a_1^\dagger - a_2^\dagger), \\ p_y &= \frac{1}{2} m\Omega \sqrt{\frac{\hbar}{m\Omega}} (a_1 - a_2 + a_1^\dagger - a_2^\dagger). \end{aligned} \quad (\text{A8})$$

Therefore, an applied alternating current (AC) electric field along x couples to the hole via the dipole term $H_{ed} = -eE_x x$. The operator x in this term can only couple the states with $\Delta n = 1$ and the same spin orientations and hence cannot achieve EDSR between the two lowest states $|0, 0, \pm 3/2\rangle$, because $\langle 0, 0, +3/2 | -eE_x x | 0, 0, -3/2 \rangle = 0$. But when we consider the SOC, the situation will be different. The SOC leads to coupling of the two lowest states $|0, 0, \pm 3/2\rangle$ to the states with the opposite spin orientations and different n , l , such as $\langle 1, -1, +3/2 | H_R | 0, 0, -3/2 \rangle \neq 0$. Thus, the two lowest states are the mixture of two opposite spin states, as expressed in Eq. (3) in the main text. With the aid of spin-orbit coupling, the electric field E_x can couple the two lowest states, i.e., $\langle 0+ | -eE_x x | 0- \rangle \neq 0$ and EDSR occurs. It is worth noting that only the SOC that couples the $|0, 0, \pm 3/2\rangle$ to the $n = 1$ excited states can generate the EDSR, because the electric field can only induce the coupling between the states with $\Delta n = 1$.

APPENDIX B: FORMULA OF RABI FREQUENCY

We now derive the formula for the Rabi frequency based on the k -linear Rashba spin-orbit coupling (SOC), following the

standard procedure as done in 2D electron gases because of the same form of SOC [22,39]. First, we perform a Schrieffer-Wolff transformation to diagonalize the total QD Hamiltonian containing SOC, i.e., $H_{QD} + H_{SO}$. This transformation removes the spin-orbit interaction in the leading order. Second, we apply the same transformation to the total Hamiltonian including E_{AC} . Third, by disregarding the spin-independent part, we obtain an effective Rabi-type Hamiltonian in the logical basis $|0+\rangle$, $|0-\rangle$,

$$H_{EDSR} = \frac{1}{2} g \mu_B \mathbf{B} \cdot \boldsymbol{\sigma} + \frac{1}{2} \delta \mathbf{B}(t) \cdot \boldsymbol{\sigma}. \quad (\text{B1})$$

Here $\delta \mathbf{B}(t)$ is the effective magnetic field induced by the combination of E_{AC} and k -linear Rashba SOC and is expressed by

$$\delta \mathbf{B}(t) = 2\mathbf{B} \times [\boldsymbol{\Omega}_1(t) + \mathbf{n} \times \boldsymbol{\Omega}_2(t)], \quad (\text{B2})$$

where $\boldsymbol{\Omega}_1 = e\alpha\lambda_1(E_y, E_x, 0)$, $\boldsymbol{\Omega}_2 = e\alpha\lambda_2(-E_x, -E_y, 0)$, $\lambda_1 = \frac{E_z^2 - (\hbar\omega_0)^2}{(\omega_+^2 - E_z^2)(\omega_-^2 - E_z^2)}$, $\lambda_2 = \frac{2E_z\hbar\omega_l}{(\omega_+^2 - E_z^2)(\omega_-^2 - E_z^2)}$, $\omega_\pm = \sqrt{\omega_0^2 + \omega_L^2} \pm \omega_L$, $\omega_L = eB_z/2m$, and $E_z = \mu_B \mathbf{g} \cdot \mathbf{B}$ refers to the Zeeman splitting with a spin quantization axis $\mathbf{n} = \mathbf{B}/B$. One observes that the effective magnetic field $\delta \mathbf{B}(t)$ is always perpendicular to \mathbf{B} . Finally, we obtain the Rabi frequency $f_R = \max[|\delta \mathbf{B}(t)|]/4\hbar$.

APPENDIX C: RABI FREQUENCY FOR THE OUT-OF-PLANE MAGNETIC FIELD

In this Appendix, we give the variation of Rabi frequency with the driving electric field, the gate electric field, and the components under the in-plane magnetic field (see Fig. 4). In order to produce the same Zeeman splitting as the in-plane magnetic field in the main text, the magnitude of the out-of-plane magnetic field is set to 0.04 T. All other parameters are the same.

[1] N. W. Hendrickx, W. I. L. Lawrie, L. Petit, A. Sammak, G. Scappucci, and M. Veldhorst, *Nat. Commun.* **11**, 3478 (2020).

[2] N. W. Hendrickx, D. P. Franke, A. Sammak, G. Scappucci, and M. Veldhorst, *Nature (London)* **577**, 487 (2020).

- [3] N. W. Hendrickx, W. I. L. Lawrie, M. Russ, F. van Riggelen, S. L. de Snoo, R. N. Schouten, A. Sammak, G. Scappucci, and M. Veldhorst, *Nature (London)* **591**, 580 (2021).
- [4] N. W. Hendrickx, D. P. Franke, A. Sammak, M. Kouwenhoven, D. Sabbagh, L. Yeoh, R. Li, M. L. V. Tagliaferri, M. Virgilio, G. Capellini, G. Scappucci, and M. Veldhorst, *Nat. Commun.* **9**, 2835 (2018).
- [5] G. Scappucci, C. Kloeffel, F. A. Zwanenburg, D. Loss, M. Myronov, J.-J. Zhang, S. De Franceschi, G. Katsaros, and M. Veldhorst, *Nat. Rev. Mater.* **6**, 926 (2021).
- [6] K. Aggarwal, A. Hofmann, D. Jirovec, I. Prieto, A. Sammak, M. Botifoll, S. Martí-Sánchez, M. Veldhorst, J. Arbiol, G. Scappucci, J. Danon, and G. Katsaros, *Phys. Rev. Res.* **3**, L022005 (2021).
- [7] K. Itoh, W. L. Hansen, E. E. Haller, J. W. Farmer, V. I. Ozhogin, A. Rudnev, and A. Tikhomirov, *J. Mater. Res.* **8**, 1341 (1993).
- [8] A. M. Tyryshkin, S. Tojo, J. J. L. Morton, H. Riemann, N. V. Abrosimov, P. Becker, H.-J. Pohl, T. Schenkel, M. L. W. Thewalt, K. M. Itoh, and S. A. Lyon, *Nat. Mater.* **11**, 143 (2012).
- [9] D. V. Bulaev and D. Loss, *Phys. Rev. Lett.* **95**, 076805 (2005).
- [10] L. Zhang, J.-W. Luo, A. Saraiva, B. Koiller, and A. Zunger, *Nat. Commun.* **4**, 2396 (2013).
- [11] M. Lodari, A. Tosato, D. Sabbagh, M. A. Schubert, G. Capellini, A. Sammak, M. Veldhorst, and G. Scappucci, *Phys. Rev. B* **100**, 041304(R) (2019).
- [12] J.-W. Luo, S.-S. Li, and A. Zunger, *Phys. Rev. Lett.* **119**, 126401 (2017).
- [13] D. V. Bulaev and D. Loss, *Phys. Rev. Lett.* **98**, 097202 (2007).
- [14] P. Szumniak, S. Bednarek, B. Partoens, and F. M. Peeters, *Phys. Rev. Lett.* **109**, 107201 (2012).
- [15] P. Szumniak, S. Bednarek, J. Pawłowski, and B. Partoens, *Phys. Rev. B* **87**, 195307 (2013).
- [16] K. Wang, G. Xu, F. Gao, H. Liu, R.-L. Ma, X. Zhang, Z. Wang, G. Cao, T. Wang, J.-J. Zhang, D. Culcer, X. Hu, H.-W. Jiang, H.-O. Li, G.-C. Guo, and G.-P. Guo, *Nat. Commun.* **13**, 206 (2022).
- [17] M. Xiao, I. Martin, E. Yablonovitch, and H. W. Jiang, *Nature (London)* **430**, 435 (2004).
- [18] F. H. L. Koppens, C. Buizert, K. J. Tielrooij, I. T. Vink, K. C. Nowack, T. Meunier, L. P. Kouwenhoven, and L. M. K. Vandersypen, *Nature (London)* **442**, 766 (2006).
- [19] M. Veldhorst, C. H. Yang, J. C. C. Hwang, W. Huang, J. P. Dehollain, J. T. Muhonen, S. Simmons, A. Laucht, F. E. Hudson, K. M. Itoh, A. Morello, and A. S. Dzurak, *Nature (London)* **526**, 410 (2015).
- [20] D. V. Khomitsky, L. V. Gulyaev, and E. Y. Sherman, *Phys. Rev. B* **85**, 125312 (2012).
- [21] D. M. Zajac, A. J. Sigillito, M. Russ, F. Borjans, J. M. Taylor, G. Burkard, and J. R. Petta, *Science* **359**, 439 (2018).
- [22] M. Borhani and X. Hu, *Phys. Rev. B* **85**, 125132 (2012).
- [23] L. A. Terrazos, E. Marcellina, Z. Wang, S. N. Coppersmith, M. Friesen, A. R. Hamilton, X. Hu, B. Koiller, A. L. Saraiva, D. Culcer, and R. B. Capaz, *Phys. Rev. B* **103**, 125201 (2021).
- [24] P. M. Mutter and G. Burkard, *Phys. Rev. Research* **3**, 013194 (2021).
- [25] V. N. Golovach, M. Borhani, and D. Loss, *Phys. Rev. B* **74**, 165319 (2006).
- [26] R. Winkler, *Spin-Orbit Coupling Effects in Two-Dimensional Electron and Hole Systems*, Springer Tracts in Modern Physics (Springer-Verlag, Berlin, 2003).
- [27] R. Moriya, K. Sawano, Y. Hoshi, S. Masubuchi, Y. Shiraki, A. Wild, C. Neumann, G. Abstreiter, D. Bougeard, T. Koga, and T. Machida, *Phys. Rev. Lett.* **113**, 086601 (2014).
- [28] J.-W. Luo, A. N. Chantis, M. van Schilfgaarde, G. Bester, and A. Zunger, *Phys. Rev. Lett.* **104**, 066405 (2010).
- [29] E. Marcellina, A. R. Hamilton, R. Winkler, and D. Culcer, *Phys. Rev. B* **95**, 075305 (2017).
- [30] Z. Wang, E. Marcellina, A. R. Hamilton, J. H. Cullen, S. Rogge, J. Salfi, and D. Culcer, *npj Quantum Inf.* **7**, 54 (2021).
- [31] J.-X. Xiong, S. Guan, J.-W. Luo, and S.-S. Li, *Phys. Rev. B* **103**, 085309 (2021).
- [32] R. Winkler, *Phys. Rev. B* **62**, 4245 (2000).
- [33] J.-W. Luo, L. Zhang, and A. Zunger, *Phys. Rev. B* **84**, 121303(R) (2011).
- [34] C. Kloeffel, M. Trif, and D. Loss, *Phys. Rev. B* **84**, 195314 (2011).
- [35] E. L. Ivchenko, A. Y. Kaminski, and U. Rössler, *Phys. Rev. B* **54**, 5852 (1996).
- [36] J.-W. Luo, G. Bester, and A. Zunger, *Phys. Rev. B* **92**, 165301 (2015).
- [37] L. E. Golub and E. L. Ivchenko, *Phys. Rev. B* **69**, 115333 (2004).
- [38] M. V. Durnev, M. M. Glazov, and E. L. Ivchenko, *Phys. Rev. B* **89**, 075430 (2014).
- [39] M. Borhani, V. N. Golovach, and D. Loss, *Phys. Rev. B* **73**, 155311 (2006).
- [40] A. J. Miller, M. Brickson, W. J. Hardy, C.-Y. Liu, J.-Y. Li, A. Baczewski, M. P. Lilly, T.-M. Lu, and D. R. Luhman, *arXiv:2102.01758*.
- [41] A. Sammak, D. Sabbagh, N. W. Hendrickx, M. Lodari, B. P. Wuetz, A. Tosato, L. Yeoh, M. Bollani, M. Virgilio, M. A. Schubert, P. Zaumseil, G. Capellini, M. Veldhorst, and G. Scappucci, *Adv. Funct. Mater.* **29**, 1807613 (2019).
- [42] S. Bosco, M. Benito, C. Adelsberger, and D. Loss, *Phys. Rev. B* **104**, 115425 (2021).
- [43] J. J. Wortman and R. A. Evans, *J. Appl. Phys.* **36**, 153 (1965).
- [44] K. Sawano, K. Toyama, R. Masutomi, T. Okamoto, K. Arimoto, K. Nakagawa, N. Usami, and Y. Shiraki, *Microelectron. Eng.* **88**, 465 (2011).
- [45] C. Morrison, P. Wiśniewski, S. D. Rhead, J. Foronda, D. R. Leadley, and M. Myronov, *Appl. Phys. Lett.* **105**, 182401 (2014).
- [46] Q. Shi, M. A. Zudov, C. Morrison, and M. Myronov, *Phys. Rev. B* **91**, 201301(R) (2015).
- [47] D. Laroche, S.-H. Huang, Y. Chuang, J.-Y. Li, C. W. Liu, and T. M. Lu, *Appl. Phys. Lett.* **108**, 233504 (2016).
- [48] T. M. Lu, Z. F. Li, D. C. Tsui, M. J. Manfra, L. N. Pfeiffer, and K. W. West, *Appl. Phys. Lett.* **92**, 012109 (2008).
- [49] M. Cardona and Y. Y. Peter, *Fundamentals of Semiconductors* (Springer, New York, 2005), Vol. 619.
- [50] J.-X. Xiong, S. Guan, J.-W. Luo, and S.-S. Li, *arXiv:2107.07681*.
- [51] A. Crippa, R. Maurand, L. Bourdet, D. Kotekar-Patil, A. Amisse, X. Jehl, M. Sanquer, R. Laviéville, H. Bohuslavskyi, L. Hutin, S. Barraud, M. Vinet, Y.-M. Niquet, and S. De Franceschi, *Phys. Rev. Lett.* **120**, 137702 (2018).

- [52] Y. Kato, R. C. Myers, D. C. Driscoll, A. C. Gossard, J. Levy, and D. D. Awschalom, *Science* **299**, 1201 (2003).
- [53] G. Dresselhaus, *Phys. Rev.* **100**, 580 (1955).
- [54] E. Rashba and E. Sherman, *Phys. Lett. A* **129**, 175 (1988).
- [55] Y. A. Bychkov and E. I. Rashba, *J. Phys. C: Solid State Phys.* **17**, 6039 (1984).
- [56] A. Zunger, *Phys. Status Solidi A* **190**, 467 (2002).